

Supporting Information

for

Dual Tuning of Second-Harmonic Generation and Rashba Spin Splitting in Chiral Hybrid Lead Halide Perovskites via Halogen Site Engineering

Qian Xu,^{1,3,4†} Xuli Cheng,^{2,7,8†} Xiyue Cheng,^{1,4,*} Lorenzo Malavasi,⁵ Marta Morana,⁶ Juan J. Aucar,^{9,10} Muskan Nabi,⁷ Gustavo A. Aucar,^{9,10} Shuiquan Deng,^{1,4} Lingyan Feng,² Wei Ren,^{2,*} and Alessandro Stroppa^{7,*}

¹ State Key Laboratory of Functional Crystals and Devices, Fujian Institute of Research on the Structure of Matter (FJIRSM), Chinese Academy of Sciences (CAS), Fuzhou, 350108, China

² Material Genome Institute, Physics Department, State Key Laboratory of Advanced Special Steels, School of Materials Science and Engineering, Shanghai Engineering Research Center for Integrated Circuits and Advance Display Materials, Institute for Quantum Science and Technology, International Center for Quantum and Molecular Structures, Shanghai University, Shanghai 200444, China

³ College of Physics and Energy, Fujian Normal University, Fuzhou, 350117, China

⁴ Fujian College, University of Chinese Academy of Sciences, Beijing, 100049, China

⁵ Department of Chemistry and INSTM, University of Pavia, Viale Taramelli 16 27100 Pavia, Italy

⁶ Dipartimento di Scienze della Terra, University di Firenze, Via La Pira, 4, 50121 Florence, Italy

⁷ CNR-SPIN, c/o Dip.to di Scienze Fisiche e Chimiche - Via Vetoio - 67100 - Coppito (AQ), Italy

⁸ Department of Materials Science and Metallurgy, University of Cambridge, 27 Charles Babbage Road, Cambridge CB3 0FS, United Kingdom

⁹ Physics Department, Natural and Exact Science Faculty; National Northeastern University of Argentina, Avda Libertad 5460, W3404AAS, Corrientes, Argentina

¹⁰ Institute for Modelling and Innovative Technology, IMIT (CONICET-UNNE), Avda Libertad 5460, W3404AAS, Corrientes, Argentina

† These authors contributed equally to this work.

Corresponding Author

* Xiyue Cheng (xycheng@fjirsm.ac.cn)

* Wei Ren (renwei@shu.edu.cn)

* Alessandro Stroppa (alessandro.stroppa@spin.cnr.it)

CONTENTS

Tables S1-S10	3
Figures S1-S9	16
References	25

Tables S1-S10

Table S1. Calculated values of E_g^{PBE} , E_g^{SOC} , E_g^{HSE} , static SHG tensor d_{ij} , effective powder SHG response d_{eff}^p at static limit and 1064 nm, and birefringence at 1064 nm for theoretical (R)-o-BrMBAPbI₃-theory.

Material	E_g^{PBE} (eV)	E_g^{SOC} (eV)	E_g^{HSE} (eV)	d_{ij} (pm/V)		d_{eff}^p (pm/V) static limit ($\omega \rightarrow 0$)	d_{eff}^p (pm/V) at 1064 nm	Δn at 1064 nm
(R)-o- BrMBAPbI ₃ -theory	2.85	2.42	3.64	$d_{14} = -0.19$ $d_{21} = -0.90$ $d_{23} = -0.45$ $d_{34} = 0.15$	$d_{16} = -0.29$ $d_{22} = -2.34$ $d_{25} = -0.14$ $d_{36} = -0.20$	1.205 ($3.65 \times d_{eff}^{\text{KDP}}$)	2.682 ($8.13 \times d_{eff}^{\text{KDP}}$)	0.112

Table S2. Bond length values after structure optimization for (S)-o-BrMBAPbI₃, as well as the experimental values from this work.

Bonds	(S)-o-BrMBAPbI ₃ Bond lengths (Å)		
	Experimental	PBE-GGA	DFT-D3
Pb1-I1	3.287	3.273	3.289
Pb1-I2	3.169	3.201	3.198
Pb1-I3	3.481	3.404	3.404
Pb1-I4	3.051	3.121	3.123
Pb1-I5	3.275	3.292	3.292
Pb1-I6	3.192	3.217	3.228
Avg.	3.242	3.251	3.256
C-C	1.421	1.427	1.427
C-Br	1.929	1.916	1.919
N-C	1.512	1.524	1.524
N-H	0.891	1.038	1.037

Table S3. Bond length values after structure optimization for (S)-m-BrMBA₂PbI₄, as well as the experimental values obtained from reference¹.

Bonds	(S)-m-BrMBA ₂ PbI ₄ Bond lengths (Å)		
	Experimental ¹	PBE-GGA	DFT-D3
Pb1-I1	3.183	3.214	3.216
Pb1-I2	3.182	3.181	3.188
Pb1-I3	3.176	3.192	3.200
Pb1-I4	3.208	3.242	3.236
Pb1-I5	3.308	3.323	3.326
Pb1-I6	3.149	3.169	3.160
Avg.	3.201	3.220	3.221
C-C	1.419	1.426	1.426
C-Br	1.902	1.907	1.910
N-C	1.511	1.512	1.511
N-H	0.910	1.043	1.043

Table S4. Bond length values after structure optimization for (S)-p-BrMBA₂PbI₄, as well as the experimental values from this work.

Bonds	(S)-p-BrMBA ₂ PbI ₄ Bond lengths (Å)		
	Experimental	PBE-GGA	DFT-D3
Pb1-I1	3.172	3.210	3.205
Pb1-I2	3.291	3.321	3.309
Pb1-I3	3.176	3.203	3.205
Pb1-I4	3.278	3.264	3.284
Pb1-I5	3.243	3.258	3.268
Pb1-I6	3.300	3.304	3.309
Pb2-I1	3.189	3.200	3.195
Pb2-I2	3.122	3.190	3.189
Pb2-I3	3.214	3.246	3.251
Pb2-I4	3.399	3.349	3.367
Pb2-I5	3.235	3.229	3.239
Pb2-I6	3.336	3.357	3.363
Avg.	3.246	3.261	3.265
C-C	1.423	1.426	1.427
C-Br	1.948	1.908	1.910
N-C	1.544	1.516	1.516
N-H	0.891	1.042	1.042

Table S5. Optimized crystal structure data for (S)-o-BrMBAPbI₃.

Lattice parameters				Space group	
$a=8.680\text{\AA}$ $b=8.058\text{\AA}$ $c=11.561\text{\AA}$ $\beta=99.83^\circ$				$P2_1$	
Atoms	x	y	z	Wyckoff sites	Occupancy
Pb	0.4937	0.5960	0.4930	$2a$	1.000
I1	0.5197	0.3668	0.7213	$2a$	1.000
I2	0.7834	0.8061	0.6049	$2a$	1.000
I3	0.7370	0.3523	0.3950	$2a$	1.000
C1	0.1553	0.3522	0.8810	$2a$	1.000
C2	0.0288	0.3672	0.7736	$2a$	1.000
C3	0.2269	0.1989	0.9129	$2a$	1.000
C4	0.2041	0.4883	0.9541	$2a$	1.000
C5	0.3174	0.4738	0.0548	$2a$	1.000
C6	0.3849	0.3189	0.0847	$2a$	1.000
C7	0.3398	0.1817	0.0134	$2a$	1.000
C8	0.9576	0.2044	0.7249	$2a$	1.000
Br	0.1148	0.7034	0.9166	$2a$	1.000
N	0.0935	0.4554	0.6756	$2a$	1.000
H1	0.9359	0.4501	0.7935	$2a$	1.000
H2	0.0136	0.4522	0.5982	$2a$	1.000
H3	0.1967	0.4003	0.6606	$2a$	1.000
H4	0.1189	0.5790	0.6956	$2a$	1.000
H5	0.1936	0.0906	0.8580	$2a$	1.000
H6	0.3527	0.5823	0.1093	$2a$	1.000
H7	0.4723	0.3066	0.1641	$2a$	1.000
H8	0.3920	0.0606	0.0365	$2a$	1.000
H9	0.0433	0.1232	0.6933	$2a$	1.000
H10	0.8625	0.2285	0.6513	$2a$	1.000
H11	0.9081	0.1379	0.7927	$2a$	1.000

Table S6. Optimized crystal structure data for (S)-m-BrMBA₂PbI₄.

Lattice parameters				Space group	
$a=9.155\text{\AA}$ $b=8.225\text{\AA}$ $c=17.778\text{\AA}$ $\beta=99.05^\circ$				$P2_1$	
Atoms	x	y	z	Wyckoff sites	Occupancy
Pb	0.7515	0.7335	0.0013	$2a$	1.000
I1	0.8388	0.6762	0.1817	$2a$	1.000
I2	0.5488	0.4165	0.9897	$2a$	1.000
I3	0.6725	0.7213	0.8196	$2a$	1.000
I4	0.9227	0.0787	0.0215	$2a$	1.000
C1	0.2718	0.6834	0.2073	$2a$	1.000
C2	0.2357	0.7081	0.2868	$2a$	1.000
C3	0.1679	0.7419	0.4350	$2a$	1.000
C4	0.2054	0.5703	0.3280	$2a$	1.000
C5	0.1723	0.5894	0.4013	$2a$	1.000
C6	0.2000	0.8783	0.3937	$2a$	1.000
C7	0.2350	0.8619	0.3204	$2a$	1.000
C8	0.4366	0.6870	0.2037	$2a$	1.000
C9	0.2174	0.6511	0.7629	$2a$	1.000
C10	0.2955	0.6994	0.6974	$2a$	1.000
C11	0.2934	0.8618	0.6733	$2a$	1.000
C12	0.3718	0.9053	0.6154	$2a$	1.000
C13	0.4511	0.7916	0.5799	$2a$	1.000
C14	0.4484	0.6294	0.6026	$2a$	1.000
C15	0.3714	0.5832	0.6610	$2a$	1.000
C16	0.0515	0.6808	0.7479	$2a$	1.000
Br1	0.1314	0.4012	0.4574	$2a$	1.000
Br2	0.3647	0.1266	0.5825	$2a$	1.000
N1	0.1931	0.8080	0.1533	$2a$	1.000
N2	0.2838	0.7432	0.8339	$2a$	1.000

Table S6. The optimized crystal structure data for (S)-m-BrMBA₂PbI₄ (continued).

Atoms	x	y	z	Wyckoff sites	Occupancy
H1	0.2257	0.5659	0.1857	2a	1.000
H2	0.0801	0.8048	0.1564	2a	1.000
H3	0.2043	0.7791	0.0977	2a	1.000
H4	0.2337	0.9260	0.1641	2a	1.000
H5	0.1412	0.7543	0.4922	2a	1.000
H6	0.2080	0.4499	0.3025	2a	1.000
H7	0.1982	0.9984	0.4196	2a	1.000
H8	0.2612	0.9706	0.2898	2a	1.000
H9	0.4582	0.6595	0.1460	2a	1.000
H10	0.4923	0.5952	0.2427	2a	1.000
H11	0.4847	0.8064	0.2206	2a	1.000
H12	0.2564	0.8663	0.8303	2a	1.000
H13	0.3991	0.7343	0.8429	2a	1.000
H14	0.2443	0.6979	0.8816	2a	1.000
H15	0.2397	0.5221	0.7766	2a	1.000
H16	0.2328	0.9544	0.6998	2a	1.000
H17	0.5128	0.8280	0.5352	2a	1.000
H18	0.5086	0.5391	0.5748	2a	1.000
H19	0.3713	0.4563	0.6789	2a	1.000
H20	0.0266	0.8097	0.7359	2a	1.000
H21	0.9999	0.6450	0.7971	2a	1.000
H22	0.0020	0.6091	0.6985	2a	1.000

Table S7. Optimized crystal structure data for (S)-p-BrMBA₂PbI₄.

Lattice parameters				Space group	
$a=12.722\text{\AA}$ $b=12.768\text{\AA}$ $c=32.749\text{\AA}$ $\beta=93.92^\circ$				C2	
Atoms	x	y	z	Wyckoff sites	Occupancy
Pb1	0.7452	0.1606	0.9987	4c	1.000
Pb2	0.7526	0.9734	0.4988	4c	1.000
I1	0.7837	0.9576	0.5979	4c	1.000
I2	0.6916	0.2298	0.5006	4c	1.000
I3	0.1859	0.9107	0.0014	4c	1.000
I4	0.7637	0.9778	0.4016	4c	1.000
I5	0.7518	0.1675	0.9010	4c	1.000
I6	0.7698	0.1344	0.0962	4c	1.000
I7	0.5000	0.0853	0.0000	2a	1.000
I8	0.5000	0.7136	0.0000	2a	1.000
I9	0.5000	0.5340	0.5000	2b	1.000
I10	0.5000	0.8963	0.5000	2b	1.000
C1	0.5140	0.2090	0.6515	4c	1.000
C2	0.8723	0.0048	0.7892	4c	1.000
C3	0.4454	0.2379	0.6813	4c	1.000
C4	0.6163	0.1762	0.6643	4c	1.000
C5	0.5784	0.1979	0.7347	4c	1.000
C6	0.6488	0.1704	0.7057	4c	1.000
C7	0.0778	0.9517	0.8173	4c	1.000
C8	0.9523	0.9995	0.7622	4c	1.000
C9	0.0553	0.9735	0.7758	4c	1.000
C10	0.4763	0.2080	0.6067	4c	1.000
C11	0.5212	0.4190	0.8887	4c	1.000
C12	0.5133	0.1137	0.5833	4c	1.000
C13	0.4632	0.3195	0.8991	4c	1.000
C14	0.8958	0.9807	0.8303	4c	1.000
C15	0.4983	0.4535	0.8448	4c	1.000
C16	0.4769	0.2329	0.7230	4c	1.000
C17	0.3863	0.8717	0.2777	4c	1.000
C18	0.6323	0.0196	0.2173	4c	1.000
C19	0.6415	0.9215	0.2359	4c	1.000
C20	0.3443	0.7792	0.2608	4c	1.000

Table S7. The optimized crystal structure data for (S)-p-BrMBA₂PbI₄ (continued).

Atoms	x	y	z	Wyckoff sites	Occupancy
C21	0.6140	0.8302	0.2143	4c	1.000
C22	0.3351	0.6896	0.2846	4c	1.000
C23	0.4155	0.7828	0.3433	4c	1.000
C24	0.3715	0.6917	0.3257	4c	1.000
C25	0.5252	0.9469	0.1097	4c	1.000
C26	0.5768	0.8381	0.1733	4c	1.000
C27	0.4633	0.7829	0.3869	4c	1.000
C28	0.5674	0.9359	0.1538	4c	1.000
C29	0.4212	0.8728	0.3191	4c	1.000
C30	0.5957	0.0260	0.1763	4c	1.000
C31	0.5646	0.7194	0.3924	4c	1.000
C32	0.4228	0.8888	0.0992	4c	1.000
Br1	0.6927	0.9149	0.2920	4c	1.000
Br2	0.3011	0.7715	0.2039	4c	1.000
Br3	0.6234	0.1852	0.7913	4c	1.000
Br4	0.9172	0.0231	0.7053	4c	1.000
N1	0.4948	0.5057	0.9178	4c	1.000
N2	0.5083	0.3079	0.5854	4c	1.000
N3	0.3856	0.7419	0.4159	4c	1.000
N4	0.6077	0.9112	0.0814	4c	1.000
H1	0.7921	0.0252	0.7784	4c	1.000
H2	0.3656	0.2642	0.6720	4c	1.000
H3	0.6716	0.1523	0.6420	4c	1.000
H4	0.7281	0.1436	0.7150	4c	1.000
H5	0.1582	0.9311	0.8280	4c	1.000
H6	0.1168	0.9680	0.7544	4c	1.000
H7	0.3897	0.2104	0.6041	4c	1.000
H8	0.5513	0.5650	0.9163	4c	1.000
H9	0.4987	0.4787	0.9476	4c	1.000
H10	0.9204	0.0383	0.9114	4c	1.000
H11	0.1065	0.9073	0.8946	4c	1.000
H12	0.4816	0.1160	0.5513	4c	1.000

Table S7. The optimized crystal structure data for (S)-p-BrMBA₂PbI₄ (continued).

Atoms	x	y	z	Wyckoff sites	Occupancy
H13	0.4833	0.0426	0.5972	4c	1.000
H14	0.5994	0.1085	0.5837	4c	1.000
H15	0.5001	0.2982	0.5540	4c	1.000
H16	0.5852	0.3322	0.5931	4c	1.000
H17	0.4572	0.3688	0.5922	4c	1.000
H18	0.4842	0.2945	0.9307	4c	1.000
H19	0.4858	0.2568	0.8786	4c	1.000
H20	0.3774	0.3293	0.8953	4c	1.000
H21	0.8318	0.9826	0.8508	4c	1.000
H22	0.4230	0.2562	0.7458	4c	1.000
H23	0.3931	0.9415	0.2590	4c	1.000
H24	0.6527	0.0904	0.2344	4c	1.000
H25	0.6207	0.7539	0.2291	4c	1.000
H26	0.8021	0.1177	0.2713	4c	1.000
H27	0.8656	0.1198	0.3435	4c	1.000
H28	0.5145	0.0305	0.1026	4c	1.000
H29	0.5547	0.7664	0.1568	4c	1.000
H30	0.4782	0.8640	0.3969	4c	1.000
H31	0.4542	0.9450	0.3323	4c	1.000
H32	0.5890	0.1026	0.1617	4c	1.000
H33	0.3624	0.6647	0.4102	4c	1.000
H34	0.3189	0.7901	0.4142	4c	1.000
H35	0.4182	0.7466	0.4458	4c	1.000
H36	0.5508	0.6368	0.3844	4c	1.000
H37	0.5990	0.7237	0.4241	4c	1.000
H38	0.6221	0.7510	0.3722	4c	1.000
H39	0.4312	0.8041	0.1038	4c	1.000
H40	0.3938	0.9028	0.0673	4c	1.000
H41	0.3630	0.9171	0.1191	4c	1.000
H42	0.6364	0.8360	0.0881	4c	1.000
H43	0.5774	0.9125	0.0513	4c	1.000
H44	0.3289	0.9636	0.9163	4c	1.000

Table S8. Contributions of individual atoms to the largest SHG component in (S)-o-BrMBAPbl₃, (S)-m-BrMBA₂Pbl₄, and (S)-p-BrMBA₂Pbl₄. A_τ is the contribution (in %) from a single atom τ , and C_A that from all atoms of the same type. $^{VB}A_\tau$ is the contribution (in %) of the VBs, and $^{CB}A_\tau$ from the CBs. The contributions from the s , p , and d states of the atom τ to of $^{VB}A_\tau$ and $^{CB}A_\tau$ are also shown. W_A refers to the number of the same type of atoms in a unit cell.

Material	Atom	W_A	A_τ	C_A	$^{VB}A_\tau$	$^{CB}A_\tau$	$^{VB}_sA_\tau$	$^{VB}_pA_\tau$	$^{VB}_dA_\tau$	$^{CB}_sA_\tau$	$^{CB}_pA_\tau$	$^{CB}_dA_\tau$
(S)-o- BrMBAPbl ₃ d_{22}	Pb	2	7.90	15.80	3.78	4.12	1.87	0.61	1.30	0.10	3.59	0.43
	I	6	8.67	52.04	6.66	2.01	-0.75	7.41	0.00	0.15	0.69	1.18
	C	16	1.10	17.59	0.32	0.78	-0.05	0.37	0.00	0.09	0.68	0.00
	Br	2	2.67	5.34	2.24	0.43	-0.22	2.47	-0.01	-0.08	-0.19	0.70
	N	2	3.15	6.29	2.80	0.34	-0.02	2.82	0.00	-0.03	0.38	0.00
	H	22	0.13	2.94	-0.03	0.17	-0.04	0.01	0.00	0.09	0.07	0.00
(S)-m- BrMBA ₂ Pbl ₄ d_{22}	Pb	2	6.85	13.69	0.77	6.08	-2.42	-0.40	3.59	0.16	5.59	0.34
	I	8	0.49	3.96	-2.04	2.53	-1.13	-0.90	0.00	0.23	1.38	0.93
	C	32	1.26	40.20	0.47	0.79	-0.05	0.52	0.00	0.20	0.60	0.00
	Br	4	4.65	18.58	1.32	3.32	-0.12	1.45	0.00	0.24	1.91	1.17
	N	4	2.83	11.31	1.82	1.01	-0.02	1.84	0.00	0.59	0.43	0.00
	H	44	0.28	12.24	0.12	0.16	0.11	0.01	0.00	0.09	0.07	0.00
(S)-p- BrMBA ₂ Pbl ₄ d_{16}	Pb	4	2.85	11.39	6.86	-4.01	6.57	-0.28	0.57	-0.10	-3.93	0.02
	I	16	3.76	60.13	3.57	0.18	-0.39	3.97	0.00	-0.16	0.22	0.12
	C	64	0.33	21.22	-0.17	0.51	-0.03	-0.14	0.00	0.11	0.40	0.00
	Br	8	1.92	15.38	-0.89	2.81	-0.03	-0.85	0.00	0.25	1.86	0.70
	N	8	-0.73	-5.86	-1.03	0.29	-0.02	-1.01	0.00	0.02	0.27	0.00
	H	88	-0.03	-2.28	-0.07	0.04	-0.06	-0.01	0.00	0.03	0.01	0.00

Table S9. Octahedral distortion parameters (β and $\Delta\beta$) for 2D (S)-o-BrMBAPbI₃^{*}, (S)-m-BrMBA₂PbI₄ and (S)-p-BrMBA₂PbI₄.

Material	β (°)	$\Delta\beta$ (°)
(S)-m-BrMBA ₂ PbI ₄	138.63, 152.69	14.06
(S)-p-BrMBA ₂ PbI ₄	145.76, 151.20, 156.41 146.00, 152.33, 153.74	10.65

The β angle (Pb–I–Pb bond angle) disparity ($\Delta\beta$)² are calculated by following equations:

$$\Delta\beta = \beta_{max} - \beta_{min}$$

*In 1D (S)-o-BrMBAPbI₃, the adjacent PbI₆ octahedra are connected via three coplanar I atoms, and therefore neither the β angle nor $\Delta\beta$ is defined.

Table S10. Crystal structure data for the samples investigated in the present paper. Data for (S)-m-BrMBA₂PbI₄ have been taken from reference¹.

	(S)-o-BrMBAPbI ₃	(S)-m-BrMBA ₂ PbI ₄	(S)-p-BrMBA ₂ PbI ₄
Formula weight	787.97	1116.96	1116.96
Wavelength (Å)	0.71073	0.71073	0.71073
Crystal system	Monoclinic	Monoclinic	Monoclinic
Space group	<i>P2</i> ₁	<i>P2</i> ₁	<i>C2</i>
Lattice parameters (Å)	<i>a</i> = 8.6940 (11)	<i>a</i> = 9.1551 (5)	<i>a</i> = 12.7224 (14)
	<i>b</i> = 8.0422 (10)	<i>b</i> = 8.2245 (5)	<i>b</i> = 12.7678 (14)
	<i>c</i> = 11.5683 (16)	<i>c</i> = 17.7782 (10)	<i>c</i> = 32.749 (4)
	<i>β</i> = 99.985 (5)	<i>β</i> = 99.051 (3)	<i>β</i> = 93.919 (5)
Cell Volume (Å ³)	796.59 (18)	1321.96 (13)	5307.1 (11)
Z	2	2	8
CCDC code	2501013	2222721	2479653

Figures S1-S9

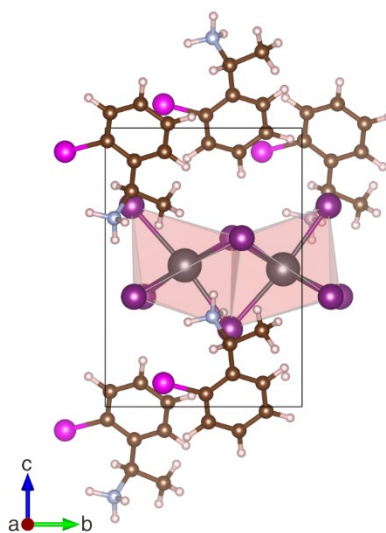


Figure S1. Crystal structures of (R)-o-BrMBAPbI₃-theory.

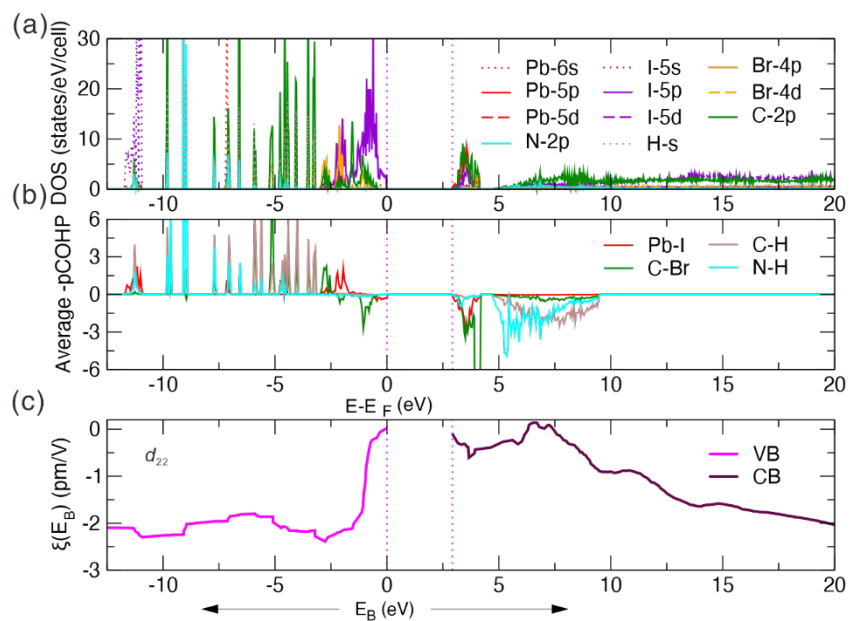


Figure S2. (a) PDOS (b) COHP analysis describing the average chemical bonding, and (c) $\zeta(E_B)$ -vs- E_B plot for the largest SHG component d_{22} of (R)-o-BrMBAPbI₃-theory.

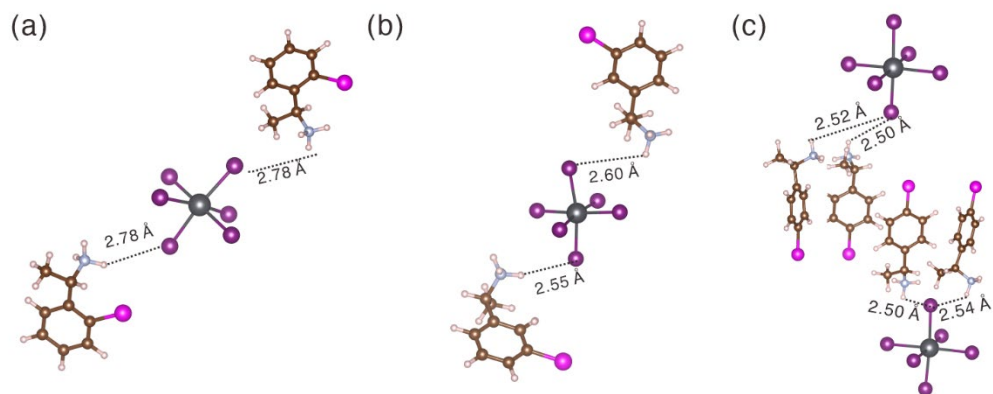


Figure S3. Coordination environments of the PbI_6 octahedra and $\text{I}\cdots\text{NH}$ weak interactions in (a) (S)-o-BrMBAPbI₃, (b) (S)-m-BrMBA₂PbI₄, and (c) (S)-p-BrMBA₂PbI₄.

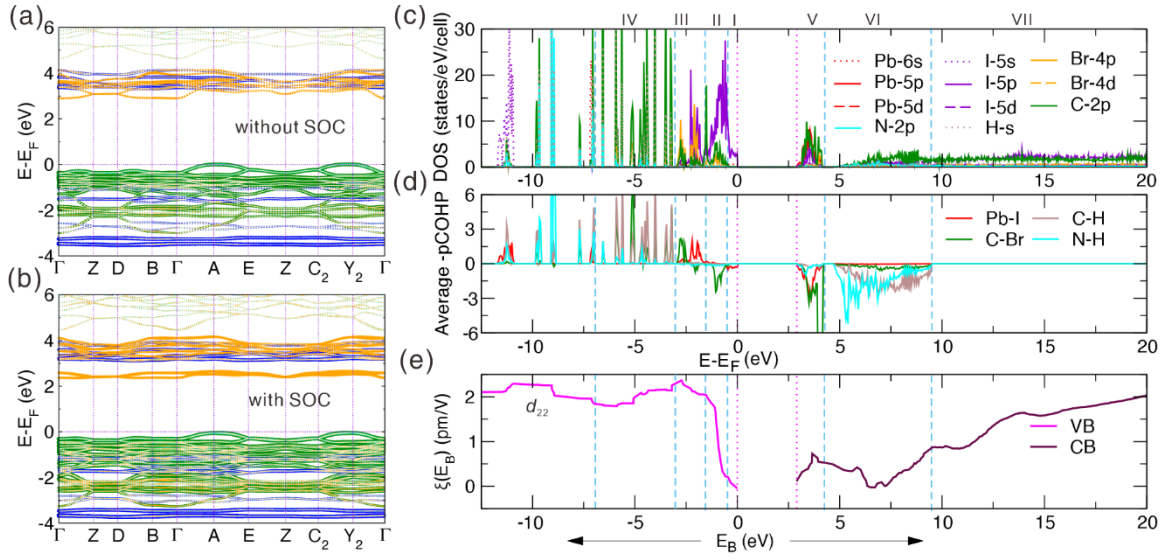


Figure S4. Electronic structures of (S)-o-BrMBAPbI₃. (a) Band structure without SOC and (b) with SOC. High-symmetry points: $\Gamma = (0, 0, 0)$, Z = (0, 0.5, 0), D = (0, 0.5, 0.5), B = (0, 0, 0.5), A = (-0.5, 0, 0.5), E = (-0.5, 0.5, 0.5), C₂ = (-0.5, 0.5, 0), and Y₂ = (-0.5, 0, 0). Key: green = I 5p; orange = Pb 6p; blue = C 2p, cyan = Pb 6s. (c) Calculated PDOS. (d) COHP analysis describing the average chemical bonding characteristics. (e) PRF analysis for the largest SHG tensor component d_{22} of (S)-o-BrMBAPbI₃.

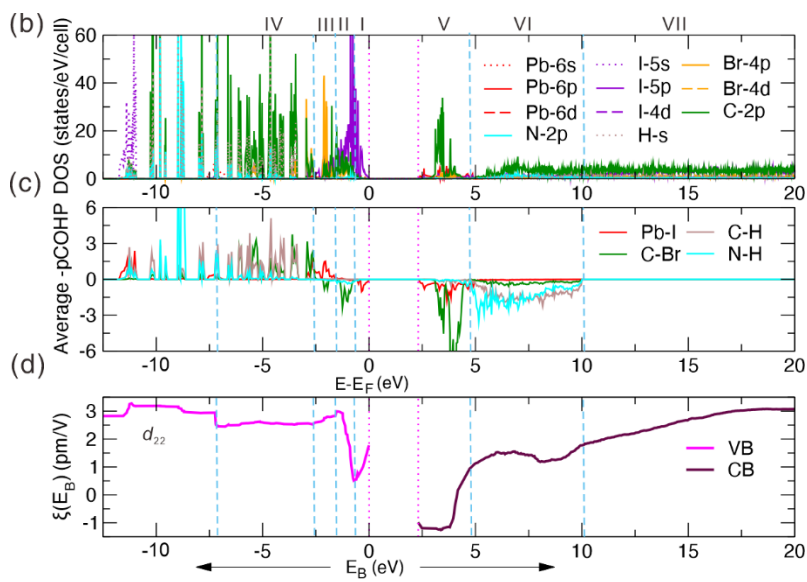


Figure S5. (a) Calculated PDOS. (b) COHP analysis describing the average chemical bonding characteristics. (c) PRF analysis for the largest SHG tensor component d_{22} of (S)-m-BrMBA₂PbI₄.

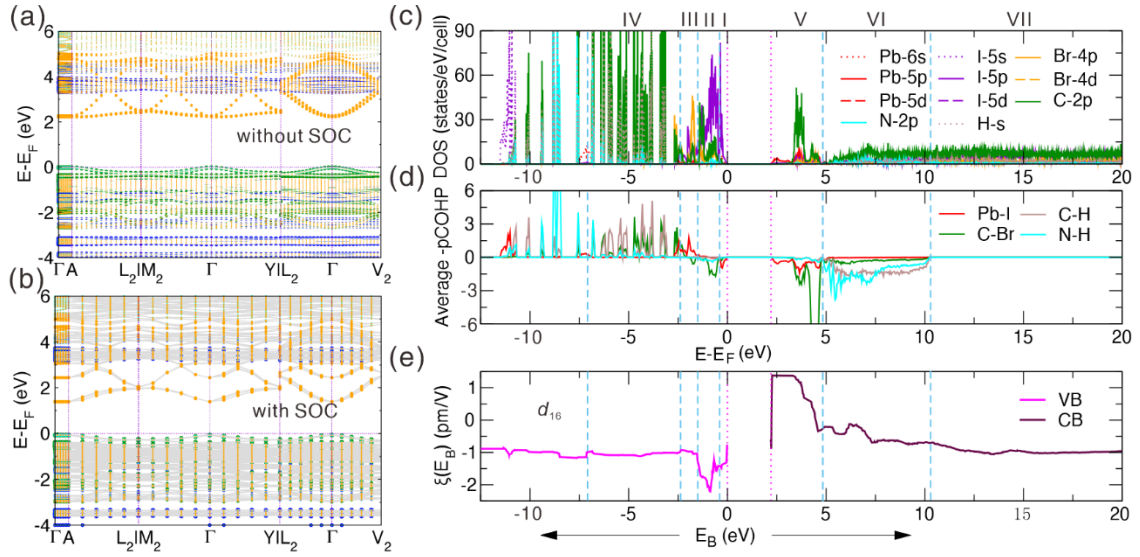


Figure S6. Band structures of (S)-p-BrMBA₂PbI₄: (a) without SOC and (b) with SOC. $\Gamma = (0, 0, 0)$, $A = (0, 0, 0.5)$, $I_2 = (0.495, 0.495, 0.5)$, $I = (-0.495, 0.504, 0.5)$, $M_2 = (-0.5, 0.5, 0.5)$, $Y = (0.5, 0.5, 0)$, $L_2 = (0, 0.5, 0.5)$, and $V_2 = (0, 0.5, 0)$. Key: green = I 5p; orange = Pb 6p; blue = C 2p, cyan = Pb 6s. (c) Calculated PDOS. (d) COHP analysis describing the average chemical bonding characteristics. (e) PRF for the largest SHG component d_{16} of (S)-p-BrMBA₂PbI₄.

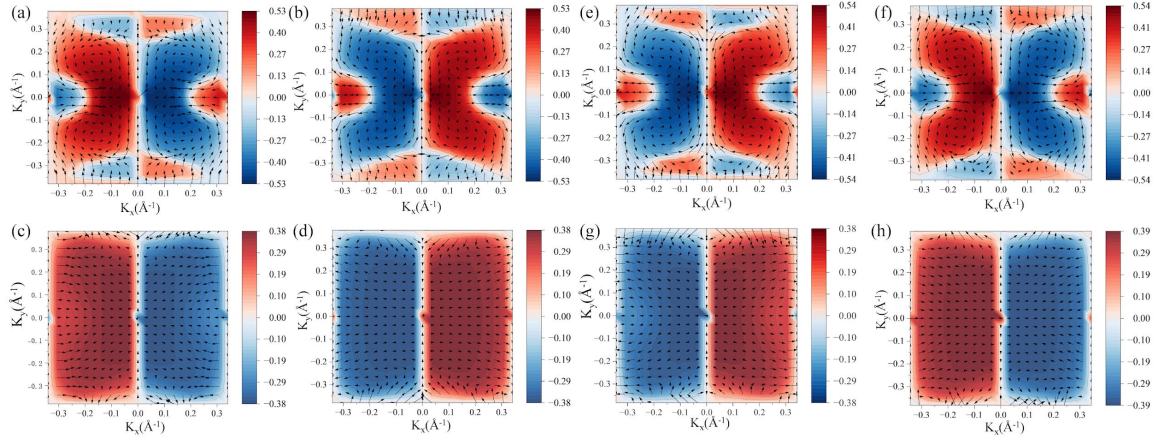


Figure S7. Spin texture of the valence and conduction band branches for (R/S)-m-BrMBA₂PbI₄. (a-d) (R)-m-BrMBA₂PbI₄: (a) outer and (b) inner VBM, (c) outer and (d) inner CBM; (e-h) (S)-m-BrMBA₂PbI₄: (e) outer and (f) inner VBM, (g) outer and (h) inner CBM. The red and blue indicate positive and negative S_z components, respectively.

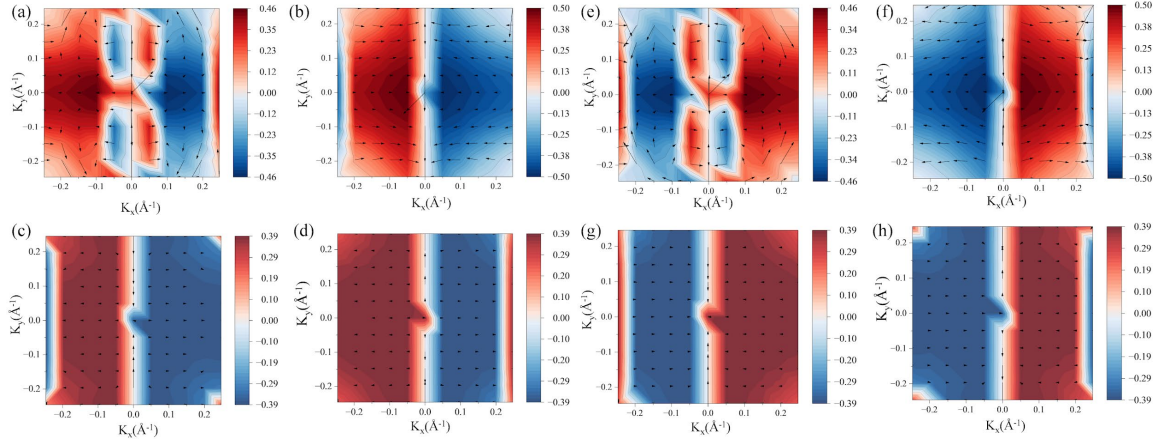


Figure S8. Spin texture of the valence and conduction band branches for (R/S)-p-BrMBA₂PbI₄. (a-d) (R)-p-BrMBA₂PbI₄: (a) outer and (b) inner VBM, (c) outer and (d) inner CBM; (e-h) (S)-p-BrMBA₂PbI₄: (e) outer and (f) inner VBM, (g) outer and (h) inner CBM. The red and blue indicate positive and negative S_z components, respectively.

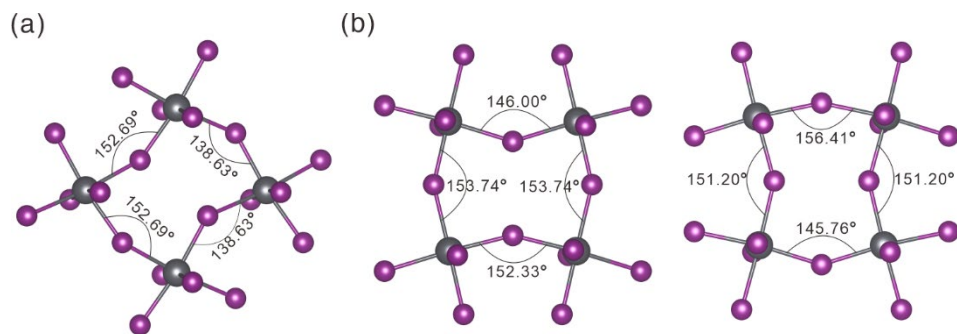


Figure S9. In-plane views of chiral OIHM perovskite layers with β angles (Pb–I–Pb bond angles) for (d) (S)-m-BrMBA₂PbI₄ and (e) (S)-p-BrMBA₂PbI₄

References

- (1) Liu, S. et al. Bright circularly polarized photoluminescence in chiral layered hybrid lead-halide perovskites. *Sci. Adv.* **9**, eadh5083 (2023).
- (2) Jana, M. K. et al. Structural descriptor for enhanced spin-splitting in 2D hybrid perovskites. *Nat. Commun.* **12**, 4982 (2021).